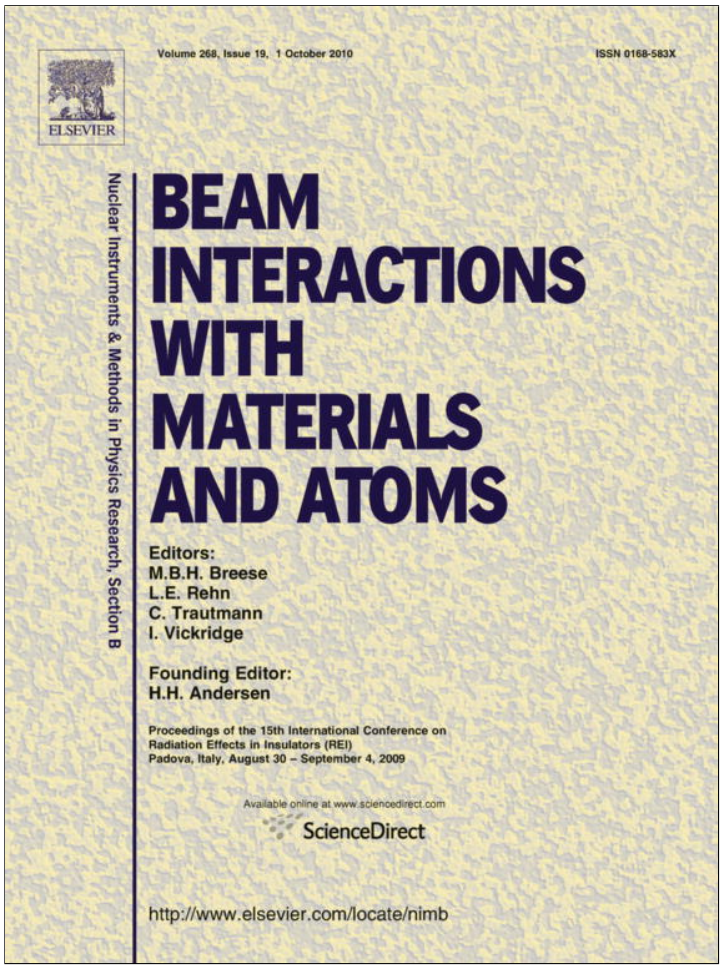

Nuclear Instruments and Methods in Physics Research B 268 (2010) 3035–3039

Contents lists available at ScienceDirect

Nuclear Instruments and Methods in Physics Research B

journal homepage: www.elsevier.com/locate/nimb

Photoluminescence from colour centres generated in lithium fluoride thin films and crystals by extreme-ultraviolet irradiation

E. Nichelatti [a,*], S. Almaviva [b], F. Bonfigli [b], I. Franzini [b], R.M. Montereali [b], M.A. Vincenti [b]

[a] ENEA C.R. Casaccia, Via Anguillarese 301, 00123 Rome, Italy
[b] ENEA C.R. Frascati, Via E. Fermi 45, 00044 Frascati, Rome, Italy

ARTICLE INFO

Article history:
Received 24 September 2009
Received in revised form 25 March 2010
Available online 16 May 2010

Keywords:
Thin film
Lithium fluoride
Colour centre
Photoluminescence
Extreme-ultraviolet

ABSTRACT

We report about the light-emitting properties of colour centres in lithium fluoride thin films and crystals treated with low-penetrating extreme-ultraviolet radiation and soft X-rays. Experimental fluorescence-imaging results show that, under the same irradiation conditions, stronger photoluminescence, up to a factor eight, is released by colour centres in a film thermally grown on silicon substrate than in a crystal. By using a classical-electromagnetism model, we take into account the role of the silicon substrate in the enhancement of spontaneous emission over a broad spectral range to analyze such behaviour.

1. Introduction

Among insulating materials, lithium fluoride (LiF) is a radiation-sensitive dielectric well known in dosimetry [1] and utilized in optoelectronic devices [2–5]. Various kinds of radiation can generate stable primary and aggregate defects, known as colour centres (CCs) [6], in LiF crystals and thin films. Some of these CCs are optically active and efficiently luminesce in the visible range at room temperature under optical pumping [6].

In the present work, we report about the light-emitting properties of CCs in LiF thin films and crystals treated with low-penetrating extreme-ultraviolet (EUV) radiation and soft X-rays. At the selected irradiation energies, a very thin (a few dozens of nanometres) surface layer of CCs is generated on the exposed face of LiF. Experimental fluorescence-imaging results show that, under the same irradiation conditions, stronger photoluminescence (PL) is released by CCs in suitable-thickness LiF films thermally evaporated on silicon (Si) substrates than in crystals [7].

To analyze the experimental results, we model light emission from CCs by means of a classical source-term theory that was first introduced by Benisty and co-workers [8,9] and further developed in recent works [10,11]. The theoretical model allows quantitatively evaluating emission from a point source or a collection of point sources embedded within whatever layered structure. Application of this model to the present case demonstrates that light emission from CCs in a LiF film over a Si substrate is enhanced with respect to what one would get in a LiF crystal. Such an enhancement is partially ascribable to the reflecting properties of the Si substrate, which provides feedback to both the optical pump and the fields radiated by CCs through constructive interference. However, the theoretical enhancement factor is not large enough to account for the measured one. The possibility that the observed larger enhancement factor could be related to a higher density of CCs in the polycrystalline film is discussed.

2. Theory

Spontaneous emission (SpE) is one of the most noticeable manifestation of the interaction of matter with vacuum: fluctuations of the vacuum electromagnetic field can induce an atomic system to decay to its ground state with the emission of photons [12,13]. In this framework, any alteration of the vacuum-field modes results in the modification of the SpE properties of atomic systems. In particular, a strong atom-vacuum coupling enhances the SpE rate, while a weak coupling inhibits it. Purcell conjectured for the first time how the SpE rate of atomic systems could be altered by the local density of vacuum-field modes in a small resonator [14]. Since then, many works have contributed to gain more and more insight into Purcell's intuition [15–26].

Despite of its inherent quantum nature, the effect of resonator boundary conditions on photon emission by an atomic system can be studied even in the realm of classical electromagnetism. In this case, the atomic system is treated as a point source,

* Corresponding author. Tel.: +39 0630484064; fax: +39 0630486364.
E-mail address: enrico.nichelatti@enea.it (E. Nichelatti).

0168-583X/$ - see front matter © 2010 Elsevier B.V. All rights reserved.
doi:10.1016/j.nimb.2010.05.034

generally consisting of a randomly-oriented dipole. In particular, light emission from inside an optical resonator consisting of a layered structure can be quantitatively evaluated by recurring to a dipole source-term theoretical model first introduced by Benisty and co-workers [8,9] and further developments achieved to evaluate anti-Stokes field generation [10] and to include effects of cooperative emission [11]. In some cases, such an evaluation can be carried out analytically [10,11], thus enabling one to quickly check the model against experimental data while varying selected parameters.

According to Benisty's model, light emission from a point source embedded in a layered medium can be evaluated by means of suitable radiating-dipole source terms and by carrying out the required calculations for multiple reflections taking place inside the layers [8,9]. This model was further developed to include volume distributions of point sources and effects of cooperative emission [11]. Analytical expressions for some selected cases can be obtained, such as the case of a homogeneous layer of atomic (molecular) systems – radiating as if they were randomly-oriented dipoles – excited by an external optical pump [11]. This configuration is suitable to describe the ultrathin layer of CCs that forms at the surface of a LiF film or crystal under EUV irradiation.

Following the source-term approach introduced in [8,9] and further developed in [11], one can write the power radiated in the outer media from a volume source embedded in a layered medium as a convenient analytical expression. The volume source is assumed to be a collection of point sources all embedded in a layer (internal layer) that is part of a multilayer. For mutually close enough point sources, the discrete distribution can be replaced by a continuous one represented by $\mu(\mathbf{r})$, where $\mathbf{r} = (x, y, z)$ is the space-position vector. According to the source-term approach, the electric field outcoupled by a single point source in a multilayer is [8,9,11]

$$E_\uparrow = \tau_\uparrow \frac{A_\uparrow + \rho_\downarrow A_\downarrow}{1 - \rho_\downarrow \rho_\uparrow}. \tag{1}$$

In this equation, $\tau_\uparrow$ and $\rho_\uparrow$ are the complex-amplitude transmittance and reflectance of the layered medium separating the point source from the outer half-space where the outcoupled field is calculated (top external medium, to fix the ideas), while $\rho_\downarrow$ is the complex-amplitude reflectance of the layered medium separating the point source from the other outer half-space (bottom external medium). All the complex-amplitude coefficients are evaluated for incidence from inside the internal layer. Eq. (1) is true for all polarization states and angles provided the complex-amplitude coefficients and the source terms are evaluated accordingly. The remaining terms are Benisty's dipole source terms [8], slightly modified to comply with our formalism [11], so that

$$A_\uparrow = A_\downarrow = \sqrt{\frac{3}{16\pi}} \tag{2a}$$

for s polarization and a horizontal dipole (that is, a dipole that lies over the Oxy plane parallel to the layer borders),

$$A_\uparrow = A_\downarrow = \sqrt{\frac{3}{16\pi}} \cos\,\theta_0 \tag{2b}$$

for p polarization and a horizontal dipole, and

$$A_\uparrow = -A_\downarrow = \sqrt{\frac{3}{8\pi}} \sin\,\theta_0 \tag{2c}$$

for p polarization and a vertical dipole (that is, a dipole that lies along the structure symmetry z axis). The propagation angle θ_0, which is measured with respect to the z axis (vertical direction) and inside the internal layer, is related to the top-external-medium propagation angle $\theta_\uparrow$ by means of Snell's refraction law. It is worth reminding that no s-polarized contribution comes from a vertically-oriented dipole. The field radiated by a point source such as a CC, seen as a randomly-oriented dipole, is built with a suitable superposition of the electric fields generated by applying Eqs. (2) to Eq. (1) [8,9,11].

Taking into account all the necessary solid-angle transformations for the propagation of the radiated powers, one can verify that the power radiated in the top external medium by a single dipole placed at z_0 within the internal layer – part of a multilayer – of refractive index n_0 and thickness d is [11]

$$w_\uparrow(z_0) = \frac{n_\uparrow^2 \cos\,\theta_\uparrow}{n_0 \cos\,\theta_0} F_\uparrow |A_\uparrow + r_\downarrow A_\downarrow \exp[-\mathrm{i}kn_0(d + 2z_0)\cos\,\theta_0]|^2. \tag{3}$$

Here, $n_\uparrow$ is the refractive index of the external medium, k is the radiation wavevector amplitude in vacuum, $r_\downarrow = \rho_\downarrow \exp[\mathrm{i}kn_0(d + 2z_0)\cos\,\theta_0]$ is the complex-amplitude reflectance, calculated for incidence from inside the layered structure, of the layers separating the internal layer from the bottom external medium, and

$$F_\uparrow = \frac{T_\uparrow}{|1 - r_\downarrow r_\uparrow \exp(-\mathrm{i}2kn_0 d\cos\,\theta_0)|^2} \tag{4}$$

is the Airy factor, where $r_\uparrow = \rho_\uparrow \exp[\mathrm{i}kn_0(d - 2z_0)\cos\,\theta_0]$ is the complex-amplitude reflectance of the layers separating the internal layer from the top external medium and $T_\uparrow$ is the intensity transmittance coefficient of the same layers, both calculated for incidence from inside the layered structure. Note that Eqs. (3) and (4) hold for both polarization states, provided the suitable polarization-dependent terms are used. The point source (randomly-oriented dipole) case is built with a proper superposition of terms obtained by Eq. (3) for the three cases of Eqs. (2).

The power outcoupled by a collection of such dipoles, assumed to be independently radiating, is just

$$W_\uparrow = \int \mu(\mathbf{r})\, w_\uparrow(z)\, \mathrm{d}^3 r, \tag{5}$$

where the integration takes place over the source volume. By substituting Eq. (3) – with z_0 replaced by z – into Eq. (5), one gets

$$W_\uparrow = \frac{n_\uparrow^2 \cos\,\theta_\uparrow}{n_0 \cos\,\theta_0} F_\uparrow \left\{ \left[|A_\uparrow|^2 + R_\downarrow |A_\downarrow|^2 \right] N + 2A_\downarrow A_\uparrow \mathrm{Re}\left[r_\downarrow \exp(-\mathrm{i}kn_0 d\cos\,\theta_0) \times \int \mu(\mathbf{r}) \exp(-\mathrm{i}2kn_0 z\cos\,\theta_0)\, \mathrm{d}^3 r \right] \right\}, \tag{6}$$

where $R_\downarrow$ is the intensity reflectance coefficient of the layers separating the internal layer from the bottom external medium, and

$$N = \int \mu(\mathbf{r})\, \mathrm{d}^3 r \tag{7}$$

is the number of dipoles in the volume.

Note that the integral expression in Eq. (6) is a three-dimensional Fourier transform of $\mu(\mathbf{r})$, which simplifies to a one-dimensional transform in case the dipole distribution depends on z only. For instance, if one assumes the internal layer to be uniformly embedded with the dipoles (uniform volume source), Eq. (6) can be verified to lead to the convenient expression

$$W_\uparrow = NT_\uparrow A_\uparrow^2 \times \frac{n_\uparrow^2 \cos\,\theta_\uparrow}{n_0 \cos\,\theta_0} \frac{1 + R_\downarrow \pm 2\sqrt{R_\downarrow}\,\mathrm{sinc}(kn_0 d\cos\,\theta_0/\pi)\,\cos(kn_0 d\cos\,\theta_0 - \Phi_\downarrow)}{1 + R_\downarrow R_\uparrow - 2\sqrt{R_\downarrow R_\uparrow}\cos(2kn_0 d\cos\,\theta_0 - \Phi_\uparrow - \Phi_\downarrow)}, \tag{8}$$

where $R_\uparrow$ is the intensity reflectance coefficient of the layers separating the internal layer from the top external medium, and $\Phi_\uparrow$ and $\Phi_\downarrow$ are the phases of $r_\uparrow$ and $r_\downarrow$, respectively. As far as the ± sign is concerned, it has be set according to the dipole orientation: plus for a horizontal dipole, minus for a vertical one.

The above-reported theory is here utilized to evaluate the photo-emission of the CCs generated in the thin surface layer of LiF as described in the following. To better model our experimental setup, the interferential effects of the laser-pump within the layered structure are properly taken into account [11] and a numerical integration over the acceptance angle of the utilized detection system is applied to Eq. (8) [10,11].

3. Sample preparation and characterization

Commercially-available LiF single crystals, typical size of $(5.0 \times 5.0 \times 0.5)\,mm^3$, polished on both sides, were used in the experiments. LiF thin films were grown by means of thermal evaporation on $(5 \times 5 \times 0.3)\,mm^3$ Si substrates in a wide range of thicknesses, extending from a few nanometres to several microns [27], at the Solid State Lasers Laboratory of ENEA C.R. Frascati. The LiF films are generally polycrystalline and their structural, morphological and optical properties strongly depend on the nature of the substrate, either amorphous or crystalline, and on the deposition parameters, in particular the substrate temperature T_s, the film total thickness and the deposition rate [27].

The LiF samples were irradiated at room temperature in vacuum ($\approx 10^{-6}$ mbar) with EUV radiation and soft X-rays generated by an excimer-pumped laser-plasma source, developed at the Excimer Laboratory of ENEA C.R. Frascati [28]. The radiation source essentially consists of solid targets, placed inside a vacuum chamber, heated by a focused powerful XeCl excimer laser operating at 308 nm, with typical pulse duration of 10–35 ns and repetition rate of 1–40 Hz. The radiation emitted by the laser-plasma source is not monochromatic. Indeed, the black-body-like emission covers the energy interval which corresponds to the full EUV range (20–300 eV) and part of the soft X-ray range (0.3–2 keV), but for the used source configuration it is centred in the EUV and only ≈10% of the emitted radiation is in the soft X-ray range.

The EUV and soft-X ray penetration depth is generally very short in solids. The method used to evaluate the depth of the coloured surface layer in our samples relies on the detailed analysis of photometric spectra of irradiated crystals recorded at the Optical Devices Laboratory of ENEA C.R. Casaccia by means of a Perkin Elmer Lambda 19 spectrophotometer, equipped with a 15 cm diameter integrating sphere, in the 210–800 nm spectral range. The analysis of the spectra was performed by applying a refractive-index model for the surface layer based on the decomposition of the total complex permeability into partial contributions of CCs, which leaded to a resulting colouration depth of about 40 nm in agreement with a Montecarlo estimation of energy deposition in LiF and further confirmed by an analytical inversion of the experimental data [29]. The analysis showed that the colouration density distribution along such a depth – very thin if compared with the wavelengths of interest – is not influent on the passive and active optical performances of the layered structure, thus allowing considering the irradiated surface layer as uniformly coloured [29].

Since a thin LiF film generally features a slightly lower density than a LiF crystal, one can wonder how much the colouration depth changes for a film. We have estimated that, in the considered energy range, a film packing density as low as 80% would increase the colouration depth from 40 nm to only about 50 nm. Therefore, we can conclude that the assumptions made here about the coloured surface layer are valid both for LiF films and crystals.

Confocal Laser-Scanning Microscopy (CLSM) images in fluorescence mode were acquired to investigate the PL properties of the irradiated LiF samples. A Nikon Eclipse 80i-C1 confocal microscope, equipped with a continuous-wave argon-ion laser Coherent INNOVA 90 operating at 457.9 nm, was used. This wavelength is located very close to the peaks of the almost overlapping absorption bands of the F_2 and F_3^+ CCs and can simultaneously excite their Stokes-shifted broad emission bands, centred at 670 nm and 535 nm, respectively [30]. The emitted PL was collected by a 20× objective (numerical aperture of 0.5) and detected by a two-channel photomultipliers system, which enables one to simultaneously acquire the green (500–530 nm) and red (650–660 nm) fluorescent signals coming from each channel, selected by suitable optical filters.

4. Results and discussion

A circular LiF film of thickness (2.20 ± 0.05) μm – measured by means of mechanical profilometry – and diameter 4 mm, thermally evaporated over a Si substrate kept at T_s = 523 K during the growth, and a LiF crystal were irradiated under identical conditions (40,000 shots at a repetition rate of 40 Hz, pulse duration 35 ns, fluence 0.025 mJ/cm^2/shot) to generate surface layers of CCs. During irradiation, the plasma temperature of the solid target (tantalum) was $\approx 3 \times 10^5$ K and the emitted radiation spectrum was peaked at ≈90 eV. A comparison between the PL signals of the irradiated film and crystal was performed by using CLSM fluorescence imaging, having care of removing stray-light contributions coming from the back-reflected laser beam that had been measured on uncoloured areas of the samples. The results are shown in Fig. 1. The photo-induced light emission coming from the LiF film on the Si substrate is significantly larger than the one coming from the LiF crystal. From the histograms in Fig. 1 (right), which show the distributions of pixel counts as functions of the signal intensity (255 levels of grey) within a selected zone of the irradiated areas, one concludes that the polycrystalline LiF film grown on Si has an average fluorescence intensity of (135 ± 9) a.u., while the LiF crystal has an average value of (16 ± 3) a.u.

The reflective properties of Si clearly help in recovering a relevant part of light emission that would be otherwise lost in the opposite direction of the observation one. This reflected part can constructively interfere with the straightly emitted one, and this is true for all the orders of multireflection at all the emission angles, provided the LiF thickness is a suitable one. Indeed, the planar structure constituted by the LiF film over the Si substrate form an elementary half-microcavity, and the thin surface layer containing CCs is located in proximity of a node of the cavity. From a quantum-optics point of view, the CCs in the LiF film are located in a thin layer where the vacuum-field modes density is increased with respect to a LiF crystal. Because spontaneous emission is stimulated by vacuum-field photons, the high vacuum-field modes density induces the colour centres in the LiF film to perform their optical cycle faster than in the LiF crystal, resulting in an increased time-averaged photon emission amount.

However, the experimentally detected higher performance of the film, corresponding to an enhancement factor of (8 ± 2) with respect to the crystal, is comparable with, but larger than, the previsions of our theoretical model. As mentioned in the previous section and in agreement with previous studies [29], the coloured volume was modelled as a surface thin layer of thickness equal to 40 nm, within which the CC density was assumed to be homogeneous. With respect to previously reported results [31], here we also include in the model the effect of the detection system numerical aperture. For the used setup of the confocal microscope – optical pumping at 457.9 nm, perpendicular to the coloured surface, emitted-light collection along the same direction (and same half-space) with numerical aperture 0.5 and allowed spectral ranges of 500–530 nm and 650–660 nm – the theoretical model foresees a PL intensity behaviour versus film thickness, for the green and red signals, as shown in Fig. 2. According to the simulated curves, the detected PL signal for a ∼2.25 μm thick LiF film is increased of ∼2.5 times for the red part of the spectrum and of

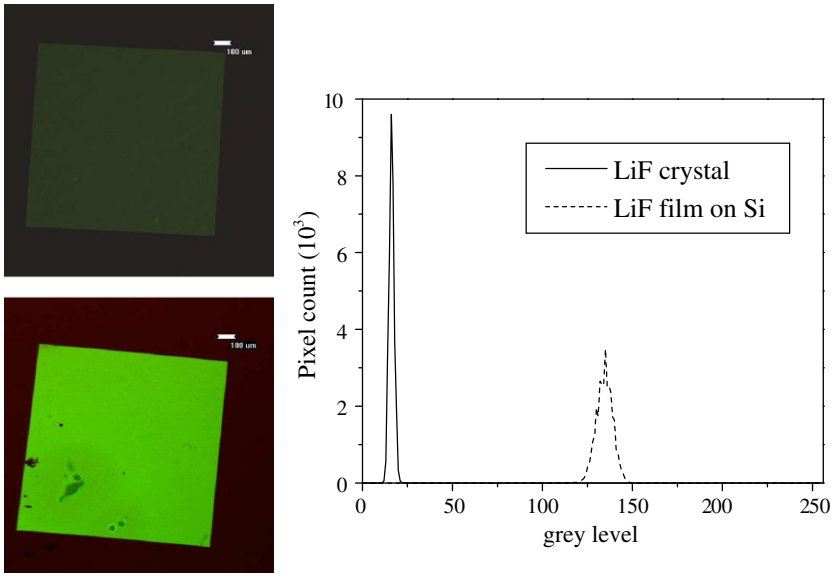

Fig. 1. Left: confocal fluorescence images of EUV-irradiated areas, masked by Si_3N_4 windows, stored in a LiF crystal (top) and in a 2.2 μm thick LiF film on a silicon substrate (bottom), irradiated under identical conditions. Bar length: 100 μm. Right: plot of the intensity distributions of the CLSM fluorescence signals, digitally acquired at 8 bit, corresponding to a reduced area in the images of the two samples.

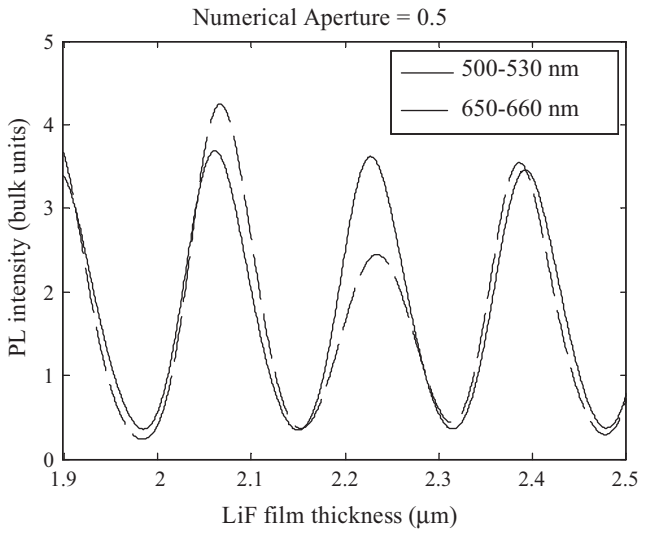

Fig. 2. Theoretical evaluation of the PL intensity radiated by a 40 nm thin surface layer of CCs over a LiF film deposited on a Si substrate and detected by an objective of numerical aperture 0.5 vs. film thickness. Intensity is normalized to the corresponding amount coming from a LiF crystal under the same irradiation and detection conditions. The detector is equipped with band-pass filters that cut radiation outside the 500–530 nm (green) and 650–660 nm (red) spectral ranges. Typical spectral distributions of PL coming from F_2 (red) and F_3^+ (green) colour centres [32] and dispersions of the material refractive indices [33,34] are taken into account.

~4 for the green one with respect to a LiF bulk. Clearly, these values are not big enough to account for the experimentally observed enhancement. To obtain the plots of Fig. 2, typical Gaussian-shaped spectral distributions of luminescence coming from F_2 (red) and F_3^+ (green) colour centres [32] and dispersions of the material refractive indices [33,34] were considered.

On the other hand, one has also to bear in mind that the formation efficiency of primary F centres and visible-emitting F_3^+ and F_2 aggregate defects is higher in polycrystalline LiF films than in single crystals and influenced by the peculiar structure of the LiF films [35]. It depends on film growth conditions, which in turn determine the surface-to-volume ratio, void presence and the preferred orientation of crystallites. It is generally accepted that the main parameters influencing CC formation are the surface-to-volume ratio and void presence as well as the direction of the irradiating beam with respect to the crystal axes. The surface-to-volume ratio and the film packing density play a relevant role because they establish the density of the grain boundaries, which act as sources of vacancies during CC formation and stabilization processes. All these effects contribute, together with the reflecting properties of Si, to explain the difference of PL efficiency between single crystals and polycrystalline films.

At the high defect densities reached in these surface layers, also concentration quenching phenomena, essentially related to interactions among the same kind of defects and/or different types of defects, could play a relevant role.

5. Conclusions

PL measurements and their comparison with theory indicate that low-penetrating EUV irradiation of LiF generates CCs with efficiencies that depend on the nature of the irradiated material, i.e., either a polycrystalline film or a monocrystalline bulk. As a matter of fact, we recorded significantly stronger PL coming from F_2 and F_3^+ CCs at the surface of a LiF film grown over a Si substrate than that coming from a crystal that had been irradiated under the same conditions. The observed enhancement factor, (8 ± 2), is too high to be barely explained by means of the optical-reflection properties of Si, hence we deduce that CCs must have formed with a larger volume density in the examined film than in the crystal.

Nonetheless, we have demonstrated that suitable thickness values of the LiF film exist for which the generated CCs result approximately located at anti-nodes of both the laser-pump and emission-field standing waves, so that the outcoupled PL results strengthened by constructive interference among internal multi-reflections. Such thickness values have to be looked for by taking into account not only the optical characteristics of the thin film, but also the features of the detecting system, such as the passing spectral bandwidths and its numerical aperture. The resulting amplification effect, strictly related to what happens in an optically-pumped microcavity, together with the higher formation

efficiency of CCs in a polycrystalline LiF film and the good spatial-resolution properties of CCs in LiF, confirm that the examined layered structure can be utilized as a convenient micro-image radiation detector [31].

Acknowledgements

Useful discussions with M. Marrocco are gratefully acknowledged. The authors are indebted with M. Montecchi, A. Faenov, F. Flora and T. Pikuz. Research carried out within FIRB-EUVL and TECVIM projects funded by the Italian Ministry of University and Scientific Research.

References

[1] A.T. Davidson, A.G. Kozakiewicz, J.D. Comins, J. Appl. Phys. 82 (1997) 3722.
[2] V.V. Ter-Mikirtychev, T.T. Tsuboi, Prog. Quant. Electr. 20 (1996) 219.
[3] R.M. Montereali, A. Mancini, G.C. Righini, S. Pelli, Opt. Commun. 153 (1998) 223.
[4] A. Belarouci, F. Menchini, H. Rigneault, B. Jacquier, R.M. Montereali, F. Somma, P. Moretti, Opt. Commun. 189 (2001) 281.
[5] K. Kawamura, M. Hirano, T. Kurobori, D. Takamizu, H. Hosono, Appl. Phys. Lett. 84 (2004) 311.
[6] W.B. Fowler, Physics of Color Centers, Academic Press, New York and London, 1968.
[7] R.M. Montereali, S. Almaviva, F. Bonfigli, A. Faenov, F. Flora, I. Franzini, E. Nichelatti, T. Pikuz, M.A. Vincenti, G. Baldacchini, Proc. SPIE 6593 (2007) 65932B-1.
[8] H. Benisty, R. Stanley, R. Mayer, J. Opt. Soc. Am. A 15 (1998) 1192.
[9] H. Benisty, H. De Neve, C. Weisbuch, IEEE J. Quantum Electron. 34 (1998) 1612.
[10] M. Marrocco, E. Nichelatti, J. Raman Spectr. 40 (2009) 732.
[11] E. Nichelatti, Cooperative Spontaneous Emission From Volume Sources in Layered Media, ENEA Technical Report RT/2009/4/FIM, ISSN/0393-3016 (2009).
[12] A. Yariv, Quantum Electronics, third ed., John Wiley and Sons, New York, 1987.
[13] P.W. Milonni, The Quantum Vacuum an Introduction to Quantum Electrodynamics, Academic Press, Boston, 1990.
[14] E.M. Purcell, Phys. Rev. 69 (1946) 681.
[15] D. Kleppner, Phys. Rev. Lett. 47 (1981) 233.
[16] F. De Martini, M. Marrocco, P. Mataloni, L. Crescentini, R. Loudon, Phys. Rev. A 43 (1991) 2480.
[17] G. Björk, S. Machida, Y. Yamamoto, K. Igeta, Phys. Rev. A 44 (1991) 669.
[18] F. De Martini, F. Cairo, P. Mataloni, F. Verzegnassi, Phys. Rev. A 46 (1992) 4220.
[19] E.F. Schubert, A.M. Vredenberg, N.E.J. Hunt, Y.H. Wong, P.C. Becker, J.M. Poate, D.C. Jacobson, L.C. Feldman, G.J. Zydzik, Appl. Phys. Lett. 61 (1992) 1381.
[20] G. Björk, H. Heitmann, Y. Yamamoto, Phys. Rev. A 47 (1993) 4451.
[21] H. Rigneault, S. Monneret, Phys. Rev. A 54 (1996) 2356.
[22] H. Rigneault, S. Robert, C. Begon, B. Jacquier, P. Moretti, Phys. Rev. A 55 (1997) 1497.
[23] O. Jedrkiewicz, R. Loudon, Phys. Rev. A 60 (1999) 4951.
[24] Y. Xu, R.K. Lee, A. Yariv, Phys. Rev. A 61 (2000) 033807.
[25] N. Danz, R. Waldhausl, A. Brauer, R. Kowarschik, J. Opt. Soc. Am. B 19 (2002) 412.
[26] N. Danz, J. Heber, A. Brauer, Phys. Rev. A 66 (2002) 063809.
[27] R.M. Montereali, Handbook of Thin Film Materials, in: H.S. Nalwa (Ed.), Ferroelectric and dielectric thin films, vol. 3, Academic Press, New York, 2002, p. 399.
[28] S. Bollanti, P. Albertano, M. Belli, P. Di Lazzaro, A. YaFaenov, F. Flora, G. Giordano, A. Grilli, F. Ianzini, S.V. Kukhlevsky, T. Letardi, A. Nottola, L. Palladino, T. Pikuz, A. Reale, L. Reale, A. Scafati, M.A. Tabacchini, I.C.E. Turcu, K. Vigli-Papadaki, G. Schina, Il Nuovo Cimento 20D (1998) 1685.
[29] R.M. Montereali, F. Bonfigli, A. Faenov, F. Flora, T. Marolo, M. Montecchi, E. Nichelatti, T. Pikuz, G. Baldacchini, Integrated Optics and Photonic Integrated Circuits, in: G.C. Righini, S. Honkanen, (Eds.), Proc. SPIE 5451, SPIE, Bellingham, WA, 2004, p. 393.
[30] J. Nahum, D.A. Wiegand, Phys. Rev. 154 (1967) 817.
[31] R.M. Montereali, S. Almaviva, F. Bonfigli, A. Faenov, F. Flora, I. Franzini, E. Nichelatti, T. Pikuz, M.A. Vincenti, G. Baldacchini, Photonic Materials Devices and Applications, in: A. Sepenguzel, G. Badenes, G.C. Righini (Eds.), Proc. SPIE 6593, SPIE, Bellingham, WA, 2007, p. 65932B_1.
[32] G. Baldacchini, E. De Nicola, R.M. Montereali, A. Scacco, V. Kalinov, J. Phys. Chem. Solids 61 (2000) 21.
[33] E. Palik, Handbook of Optical Constants of Solids, Academic Press, San Diego, 1985.
[34] E. Palik, Handbook of Optical Constants of Solids II, Academic Press, San Diego, 1991.
[35] G. Baldacchini, M. Cremona, G. d'auria, S. Martelli, R.M. Montereali, M. Montecchi, E. Burattini, A. Grilli, A. Raco, Nucl Instrum. Meth. Phys. Res. B 116 (1996) 447.